

Haptic Telemanipulation in Extensive Remote Environments

Angelika Peer, Ulrich Unterhinninghofen, Kwang-Kyu Lee, Bartłomiej Stanczyk, Martin Buss

*Institute of Automatic Control Engineering (LSR),

Technische Universität München

D-80290 Munich, Germany

Email: {angelika.peer, ulrich.unterhinninghofen, kk.lee, stanczyk, mb}@tum.de

Abstract. We present a telepresence system with visual and haptic feedback for a telemanipulation task in full six degrees-of-freedom. The employed teleoperator consists of an anthropomorphic manipulator arm mounted on a mobile base to allow task execution in wide remote environments. On the operator side we use a hyper-redundant force-reflecting input device. Control issues of operator and teleoperator and the coupling between them is discussed. Experimental results validate the approach.

Keywords. *Telepresence, Haptic Display, Mobile Robot*

I. INTRODUCTION

A telepresence system can be used to perform tasks in a distant, dangerous or badly accessible environment. Intuitive operation is achieved by tracking the motions of a human user at the operator site, replicating these motions by a telemanipulator at the remote site and transferring sensor data back to the human. In a multi-modal telepresence this principle is applied to visual, acoustic, and haptic interaction (see Fig. 1).

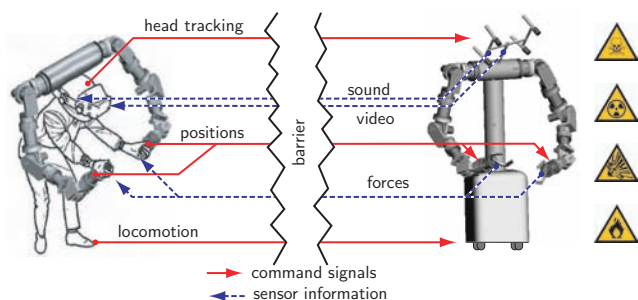


Fig.1: Teleoperation robotic system

Visual Feedback: Visual data is collected by a stereo camera head and presented to the operator via a head-mounted display (HMD) [1]. The gaze direction of the robotic head is adjusted according to the orientation of the operator's head which is measured by a tracking system. Using this setup the user can intuitively look around in the remote environment just by turning his/her own head.

Acoustic Feedback: The robotic head is equipped with two microphones placed on each side of the head. The audio data is transmitted to the operator site and reproduced via stereo headphones.

Haptic Feedback: In manipulation tasks the sensation of interaction forces is of high importance to allow dexterous operations. This is achieved by use of haptic displays which enable bidirectional human system interactions via the sense of touch. The haptic display acquires the position of the operator's hand and relays it to

the telemanipulator. In turn the resulting contact forces in the remote environment are transmitted back to the operator site where they are displayed to the user.

Existing telepresence systems are often limited to visual and acoustic feedback thus rendering real immersion into the remote environment impossible. Moreover solutions with force feedback are often restricted to a few degrees-of-freedom (DOF), low interaction forces or a strongly limited workspace. Here we present a telepresence system with visual, acoustic and haptic feedback which allows telemanipulation with two arms in full 6 DOF. The telemanipulator is placed on a mobile platform, therefore it can move around and operate in an arbitrarily large remote environment.

In section II. design and control issues of telemanipulator, haptic display and mobile base will be discussed. Experimental results will be shown in section III. We will conclude with section IV. and present an outlook to future research directions.

II. DESIGN AND CONTROL

A. Teleoperator

The superior manipulation-dexterity of human is owing to the kinematic redundancy of human arms. As many technical design solutions being inspired by nature, the bi-manual teleoperator is also anthropomorphically designed. Each arm consists of two spherical joints with 3 DOF at shoulder and wrist, respectively, and one revolute joint at elbow, which results in 7 DOF. For details about kinematic model of the teleoperator, see [2]. Comparing to a conventional 6 DOF anthropomorphic arm with spherical wrist, it is simply extended by adding a revolute joint for the elbow. Such a redundant DOF can be exploited for many attractive features such as collision avoidance, maximizing the distance from joint limits or manipulability measure, etc. Each performance criterion can be optimized separately, or multiple criteria can be taken into account simultaneously through appropria-

te combination of concerned performance measures with intelligently devised weighting factors.

A.1. Collision Avoidance

As opposed to conventional motion control in which collision avoidance has been solved on the level of task trajectory planning, for the telemanipulation of the mobile-based bi-manual teleoperator, various collision situations, for example, arm to arm, arm to its own end-effector or arm to its own body can be issued since the desired trajectory is generated by a human user and both arms share partially common workspace. Therefore, it is of practical importance to ensure avoiding such collisions online. One of the most intuitive realizations of the collision avoidance can be achieved by imitating magnetic potential field. Each arm and its subcomponents have their own potential field so that, when arbitrary two components come close together, a resulting repulsive force is generated inversely proportional to the shortest distance between them as

$$F_v(d) = \begin{cases} F_M & \text{for } d < d_m \\ F_M \frac{d_m^2(d_M-d)}{d^2(d_M-d_m)} & \text{for } d_m \leq d \leq d_M \\ 0 & \text{for } d > d_M \end{cases}, \quad (1)$$

where F_v is the magnitude of virtual force and design parameters F_M , d , d_M , and d_m are maximum virtual force, the shortest distance between concerned objects and its maximum and minimum allowable values, respectively. The virtual force is parallel to the shortest line between the two objects. When the current shortest distance d is large enough ($d > d_M$), no virtual force is generated. Inversely, when two objects are close enough ($d < d_m$), the maximum virtual force is generated.

The virtual force is added to physical interaction forces measured by the force-torque sensor and sent to the haptic display to prevent a human user from driving the teleoperator to a collision unintentionally.

Such an artificial potential concept can also be used for redundancy resolution in that the null space motion can be optimized to maximize the collision distance d or to minimize the virtual force F_v .

A.2. Position Based Impedance Control

In most teleoperation applications, the teleoperator is required to handle interactions appropriately with unstructured rigid environments. In this case, it is of practical importance to guarantee stable interactions with various types of environments. One of the most promising interaction control schemes is the position-based impedance control, see Fig. 2. Unlike explicit force control schemes that handle contact force directly, impedance control regulates the dynamics between the measured contact force and the position trajectory. So the desired trajectory which is generated by human user in the teleoperation applications, is modified according to the

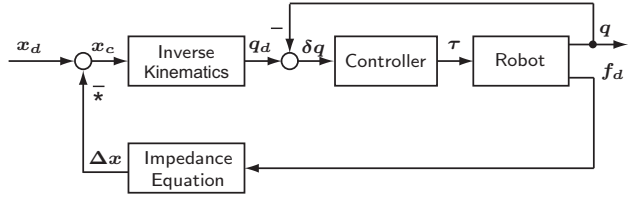


Fig.2: Position based impedance control

current measured force \mathbf{f} and moment $\boldsymbol{\mu}$ using the target impedance relation:

$$\mathbf{f} = \mathbf{M}_T \Delta \ddot{\mathbf{p}} + \mathbf{D}_T \Delta \dot{\mathbf{p}} + \mathbf{K}_T \Delta \mathbf{p}, \quad (2)$$

$$\boldsymbol{\mu} = \mathbf{M}_R \dot{\boldsymbol{\omega}} + \mathbf{D}_R \boldsymbol{\omega} + \mathbf{K}_R \boldsymbol{\epsilon}, \quad (3)$$

where \mathbf{M} , \mathbf{D} and \mathbf{K} are virtual inertia, damping and stiffness matrices, which characterize the desired target impedance of the teleoperator; subscripts 'T' and 'R' denote translational and rotational direction, respectively; $\Delta \mathbf{x}$ is the amount of modification of the desired trajectory according to the measured contact force $\mathbf{f}_d = [\mathbf{f}; \boldsymbol{\mu}]$. It comprises the position modification $\Delta \mathbf{p}$ and the orientation modification $\boldsymbol{\epsilon}$ which is the vector part of the unit quaternion representing the orientation error. Using unit quaternions to represent orientation errors allows global parametrization of orientation not suffering from the representation singularity. Furthermore, the following relations are exploited in (3):

$$\mathbf{K}_R = 2\mathbf{E}^T(\eta, \boldsymbol{\epsilon}) \mathbf{K}'_R, \quad (4)$$

$$\mathbf{E} = \eta \mathbf{I} - \mathbf{S}(\boldsymbol{\epsilon}), \quad (5)$$

where η is the scalar part of the unit quaternion, \mathbf{K}'_R is the virtual stiffness matrix in cartesian space and $\mathbf{S}(\boldsymbol{\epsilon})$ denotes the skew-symmetric matrix based on the orientation error $\boldsymbol{\epsilon}$. The rotational velocity and the unit quaternion are related by the quaternion propagation rule [3]

$$\dot{\eta} = -\frac{1}{2} \boldsymbol{\epsilon}^T \boldsymbol{\omega}, \quad (6)$$

$$\dot{\boldsymbol{\epsilon}} = \frac{1}{2} \mathbf{E}(\eta, \boldsymbol{\epsilon}) \boldsymbol{\omega}. \quad (7)$$

B. Haptic Display

In order to enable an intuitive telemanipulation the hyper redundant haptic display ViSHaRD10 (**V**irtual **S**cenario **H**aptic **R**endering **D**evice with **10** actuated DOF) is used. Its main characteristics are a very large workspace free of singularities, a high payload capability to accommodate various application specific end-effectors, foreseen redundancy to avoid kinematic singularities and user interferences and the possibility for dual-arm haptic interaction with full 6 DOF. While details about the design concept and the kinematic model of ViSHaRD10

can be found in [4], the following sections deal with the control and the inverse kinematics algorithm used in the telemanipulation experiments.

B.1. Control scheme

The haptic simulation of a human’s bilateral interaction with a remote environment requires the control of the motion-force¹ relation between operator and robot. This can be achieved by either controlling the interaction force of the device with the operator (impedance display mode) or the device motion (admittance display mode).

Admittance control is particularly well suited for robots with hard non-linearities and large dynamic properties compared to the environment being emulated. In this display mode forces are measured and motion is commanded, i. e. the robot acts as admittance and the human as impedance. Accordingly, a force sensor is required for admittance control. Contrary to haptic displays driven in the impedance mode all admittance control implementations aim at forming the closed-loop inertia. The high gain inner control loop closed on motion allows for an effective elimination of nonlinear device dynamics as for instance friction. It is thus possible to render an isotropic closed-loop dynamic behavior in order to provide the operator with a more “natural feeling“. The drawbacks are a reduced capability for the display of low impedances and a decreased closed-loop bandwidth of the force feedback. A more detailed analysis of haptic control schemes is given in [5].

In order to provide an effective compensation of disturbances due to friction and to be able to render inertia and mass admittance control is implemented as illustrated in Fig. 3. The interaction force \mathbf{f}_{ext} of the operator is measured by a force-torque sensor. According to the desired dynamics this force is related to the reference end-effector velocity $\dot{\mathbf{x}}_r$. An algorithm for inverse kinematics resolution calculates the reference joint velocities $\dot{\mathbf{q}}_r$. Alternatively, the mapping of the end-effector to the joint motion can be realized at the position or acceleration level. The joint angles \mathbf{q}_r are the reference input to a conventional position control law, e.g. a computed torque scheme [6].

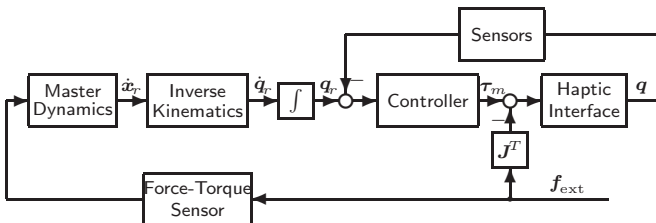


Fig.3: Admittance control scheme

¹Throughout the paper force stands for both, linear force and torque, while motion in terms of a generalization of position, velocity, and acceleration refers to both, translational and angular motion quantities.

B.2. Inverse kinematics

The mapping

$$\dot{\mathbf{x}} = \mathbf{J}\dot{\mathbf{q}} \quad (8)$$

relates the joint velocity $\dot{\mathbf{q}} \in \mathbf{R}^n$ to the end-effector velocity $\dot{\mathbf{x}} \in \mathbf{R}^m$, where \mathbf{J} is the $m \times n$ Jacobian matrix of the manipulator. If $n > m$ the manipulator is said to be redundant with respect to the end-effector task. Such a system allows for a change of the internal configuration without changing the position and orientation of the end-effector so that the redundant DOF can be used to avoid interior singularities and enable collision avoidance with the environment and the human operator. In this case a solution to the inverse kinematics problem, the calculation of $\dot{\mathbf{q}}$ from $\dot{\mathbf{x}}$, is not uniquely determinable as there are fewer equations than unknowns. To solve this problem a so called *Partitioned inverse kinematic solution*, a combination of two different inverse kinematics algorithms, *Inverse function* and *Pseudoinverse control*, is investigated.

Pseudoinverse control: A solution to (8) proposed by Liegeois [7] that applies the Moore-Penrose generalized inverse $\mathbf{J}^\#$ of the Jacobian matrix is

$$\dot{\mathbf{q}} = \mathbf{J}^\# \dot{\mathbf{x}} + [\mathbf{I} - \mathbf{J}^\# \mathbf{J}] \dot{\mathbf{q}}_0, \quad (9)$$

where the first term is the minimum norm joint velocity solution and $[\mathbf{I} - \mathbf{J}^\# \mathbf{J}] \dot{\mathbf{q}}_0$ the homogeneous solution of (8) to project an arbitrary joint velocity vector $\dot{\mathbf{q}}_0$ onto the nullspace of \mathbf{J} . The homogeneous solution can be used to improve the device performance when choosing $\dot{\mathbf{q}}_0$ to optimize a performance criterion $H(\mathbf{q})$, a scalar function of the joint angles. Using gradient projection the redundancy can then be solved by substituting $\dot{\mathbf{q}}_0$ with $\alpha \nabla H(\mathbf{q})$ resulting in

$$\dot{\mathbf{q}} = \mathbf{J}^\# \dot{\mathbf{x}} + [\mathbf{I} - \mathbf{J}^\# \mathbf{J}] \alpha \nabla H(\mathbf{q}). \quad (10)$$

In order to avoid singularities the manipulability index $m = m(\mathbf{J})$ as reported in [4] has been chosen as a performance criterion .

Inverse function: Another approach to solve the redundancy is to define a single inverse function giving the joint coordinates for each point in a specified subset of the end-effector space. In contrast to pseudoinverse control these algorithms are cyclic (every closed path in the end-effector space is tracked only by closed paths in the joint space) avoiding unpredictable joint motions. A simple inverse function can be defined when controlling the SCARA segment and joint 6 and 7 to mimic the operation of three prismatic joints:

$$\theta_1 = \arccos \frac{y}{2l_1} + \frac{\pi}{2}, \quad \theta_2 = -2\theta_1 + \pi, \quad (11)$$

$$\theta_3 = \arccos \frac{x}{2l_3} - \theta_1 - \theta_2, \quad \theta_4 = -2 \arccos \frac{x}{2l_3}, \quad (12)$$

$$\theta_6 = -\arccos \frac{z}{2l_6}, \quad \theta_7 = -2\theta_6, \quad (13)$$

where x, y, z is the end-effector position respective the base coordinate system. Setting joint angle 5 to $\theta_5 = \theta_{5,0} - \sum_{i=1}^4 \theta_i$ a unique solution to the inverse kinematics problem for the translational movement can be determined.

Using the above mentioned *Inverse function* for the translational and the *Pseudoinverse control* for the remaining rotational movement of ViSHaRD10 a decoupling of the translational from the rotational motion can be achieved. Under this assumptions and considering $\mathbf{q}_{\text{rot}}^T = [\theta_5^* \ \theta_8^* \ \theta_9 \ \theta_{10}]$ with $\theta_5^* = \theta_5 + \sum_{i=1}^4 \theta_i$ and $\theta_8^* = \theta_8 + \sum_{i=6}^7 \theta_i$ Eq.10 becomes

$$\dot{\mathbf{q}}_{\text{rot}} = \mathbf{J}_{\text{rot}}^\# \boldsymbol{\omega} + [\mathbf{I} - \mathbf{J}_{\text{rot}}^\# \mathbf{J}_{\text{rot}}] \alpha_{\text{rot}} \nabla H_{\text{rot}} \mathbf{q}_{\text{rot}}. \quad (14)$$

Here $\boldsymbol{\omega}$ is the rotational Cartesian velocity command and $\mathbf{J}_{\text{rot}} \in \mathbf{R}^{3 \times 4}$ the Jacobian relating \mathbf{q}_{rot} to $\boldsymbol{\omega}$.

C. Mobile Base

The mobile base enables the user to freely move around the teleoperator in the remote environment. In order to make these movements intuitive the mobile platform must have locomotion capabilities similar to those of a human. Therefore we use an omnidirectional platform which is operated in velocity control mode. As the operator uses both arms to control the telemanipulator arms the desired velocity is input via a foot pedal.

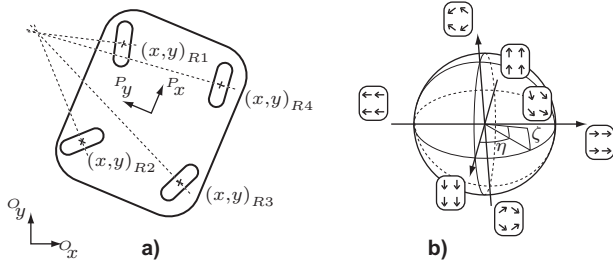


Fig. 4: (a) Kinematic model of the mobile platform
(b) Unit sphere representation of wheel configurations

The platform shown in Fig. 4a possesses four independently driven and steered wheels. Hence it comprises eight independent control inputs, whereas the platform position has only three degrees-of-freedom (two translational, one rotational). This redundancy can be resolved by taking the following conditions for obtaining an admissible wheel configuration into account: for pure translational movements the revolution axes of all modules must be parallel and the driving speeds must be equal, for all other movements the revolution axes must intersect in one single point and the driving speeds must be proportional to the distance from this intersection point. In [8] it has been proposed to represent admissible wheel configurations on a unit sphere by a set of two coordinates ζ and η . In Fig. 4b coordinates for pure rotational, pure translational and mixed motions are depicted.

The platform velocity $\dot{\mathbf{x}}$ can be fully describe by ζ, η and a generalized velocity $\boldsymbol{\omega}$:

$$\dot{\mathbf{x}} = \begin{pmatrix} \dot{x} \\ \dot{y} \\ \dot{\psi}/\kappa_G \end{pmatrix} = \boldsymbol{\omega} \begin{pmatrix} \cos \zeta \cos \eta \\ \cos \zeta \sin \eta \\ \sin \zeta \end{pmatrix}, \quad (15)$$

where κ_G is a scaling factor of dimension m^{-1} .

From the coordinates of the admissible wheel configuration the desired angle φ_i and speed v_i for each wheel $i \in \{1 \dots 4\}$ can be calculated by solving

$$v_i \begin{pmatrix} \cos \varphi_i \\ \sin \varphi_i \end{pmatrix} = \boldsymbol{\omega} \begin{pmatrix} \cos \zeta \cos \eta - \kappa_G y_{Ri} \sin \zeta \\ \cos \zeta \sin \eta - \kappa_G x_{Ri} \sin \zeta \end{pmatrix}. \quad (16)$$

The complete control structure of the mobile base is shown in Fig. 5. In the first step an admissible wheel configuration is calculated for the desired velocity input. Using this wheel configuration and the generalized velocity the control inputs to the four independent wheel controllers are generated. Steering angles and driving speeds are finally controlled by pure linear controllers.

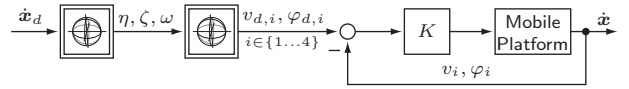


Fig. 5: Control structure of the mobile platform

D. Teleoperation control architecture

Fig. 6 shows a diagram of the implemented teleoperation control which combines the control of haptic display and teleoperator to a two-channel force position architecture. While for the haptic display admittance control as mentioned in section B. is implemented the teleoperator is controlled in impedance mode (see section A). Desired positions are sent to the teleoperator and the measured interaction forces are fed back to the operator site. In order to reduce complexity Fig. 6 can be simplified considering perfect position tracking ($\mathbf{x}_m = \mathbf{x}_r, \mathbf{x}_s = \mathbf{x}_c$) of both devices.

Under this assumption Fig. 7 can be derived. One can see that in contact, as a result of the impedance control, the reference position of the teleoperator will be modified according to Eq. 2 and 3. Consequently, transparency will be influenced by the parameter settings of the slave impedance control. The stiffer the impedance control of the slave the smaller the position deviation and the better the real environmental impedance is reproduced.

Transparency is also affected by the master control since the minimum target inertia of the haptic display is bounded by stability. In free space motion a minimal mass and inertia necessary for stability of the master control can be felt.

The stability of the overall system is guaranteed in conformity to the passivity theorem, see [9]. According to it,

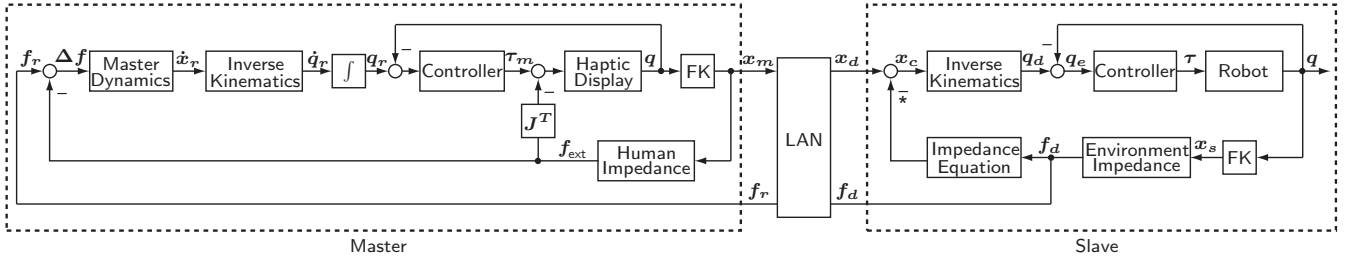


Fig. 6: Teleoperation control architecture

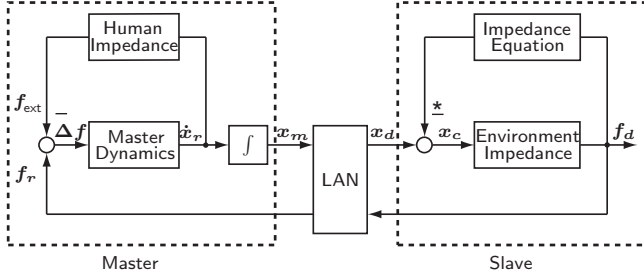


Fig. 7: Simplified teleoperation control architecture

a system consisting of passive elements is also passive. The mechanical impedance/admittance of the manipulators as well as the environment used in the experiments are passive. It is also assumed that the human operator behaves in a cooperative i.e. passive way. The only potentially non passive element is the communication network. However, in the presented experiment, the delay introduced by the internal lab network may be neglected. For a case of considerable time delay (also variable), the passivation techniques successfully implemented in our previous works [9] may be used.

III. EXPERIMENTAL RESULTS

The experimental setup consists of the haptic input device VisHaRD10 [4], the 7DOF slave manipulator and a stereo vision system. According to the bilateral control structure, the motion of the operator is read by the master device and sent as desired positions to the slave impedance controller. The measured contact forces are sent back as the input to the master admittance controller. The devices communicate over the UDP network with a sampling rate of 1kHz, which is the same as for the local loop control.

The vision system consists of two CCD cameras placed on a 3DOF camera head. The recorded video streams are displayed on the head mounted display (HMD) carried by the operator. The HMD has a built in tracker, which is used for controlling the motion of the camera head. Such a setup provides the operator with a realistic visual information about the location of the objects, the environment, and the telemanipulator. Here the anthropomorphic construction of the telemanipulator plays an

important role: the operator can drive it as if it were his/her own arm. The visual information is useful not only for motion generation, but also for handling the contact and minimizing the effects of impact.

The experiment consists of three tasks:

- tracking of free space motion
- haptic exploration of different materials (soft and stiff), see Fig. 8a
- driving a screw with an aluminium tool, see Fig. 8b. This last experiment consists of three phases: contact with extreme stiff materials, a classic peg-in-hole operation and manipulation in a constrained environment.

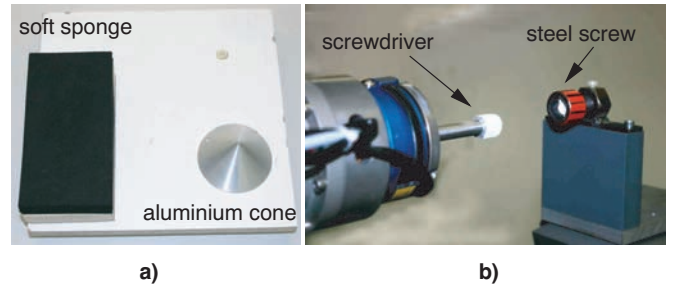


Fig. 8: Slave side: a) different materials for haptic exploration b) the screw and the screwdriver

Fig. 9 and Fig. 10 show the position and force tracking performance during haptic exploration of different materials (see Fig. 8a). The shaded areas indicate the several contact phases. One can see that during free space motion the position tracking of the slave arm works very well, while in the contact situation, as a consequence of the implemented impedance controller, the slave position differs from the master position. Please note, that as the force tracking is very good, this position displacement influences the displayed and felt environmental impedance in such a way that hard objects are perceived softer than they are. As the master controller is of admittance type, which reacts on the human force input, non zero forces during free space motion are necessary to change the actual end-effector position.

Similar results can be achieved in the screwing experiments. Although screwing differs from the simple exploration scenario as more than one translational and rotational constraint is active at the same time a quite small

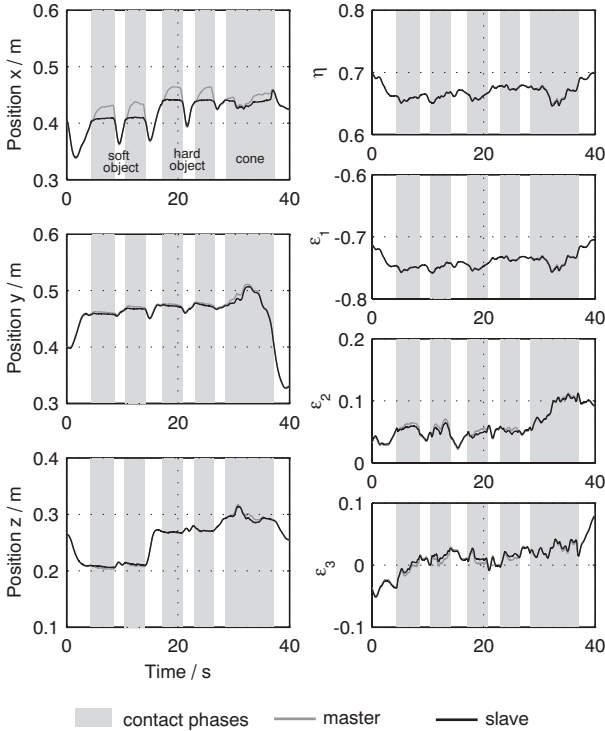


Fig.9: Position tracking (Slave) during haptic exploration

position displacement and a very good force tracking in all translational and rotational directions can be achieved. The active compliance introduced by the impedance control of the slave arm emulates a human like compliant behavior when interacting with the environment and enables screwing without destruction of screw and environment.

IV. CONCLUSIONS

We have presented a multi-modal telepresence system which allows dexterous teleoperation in large remote environments. Kinematic redundancies of teleoperator and haptic displays have been exploited in order to avoid collisions and internal singularities. The control algorithm of the mobile platform provides human-like motion capabilities without pre-planned paths. Experiments have shown the suitability of the developed system for operations requiring all 6 DOF. Future research will aim at enlarging the existing system for bimanual and collaborative telemanipulation tasks. Furthermore we will equip the manipulator arms with robotic hands which will make more complex assignments e.g. grasping tasks possible.

ACKNOWLEDGMENTS

This work is supported in part by the German Research Foundation (DFG) within the collaborative research center SFB453 project. Special thanks go to J. Gradl, H. Kubick, T. Lowitz and T. Stoeber for their excellent work during the robot construction phase.

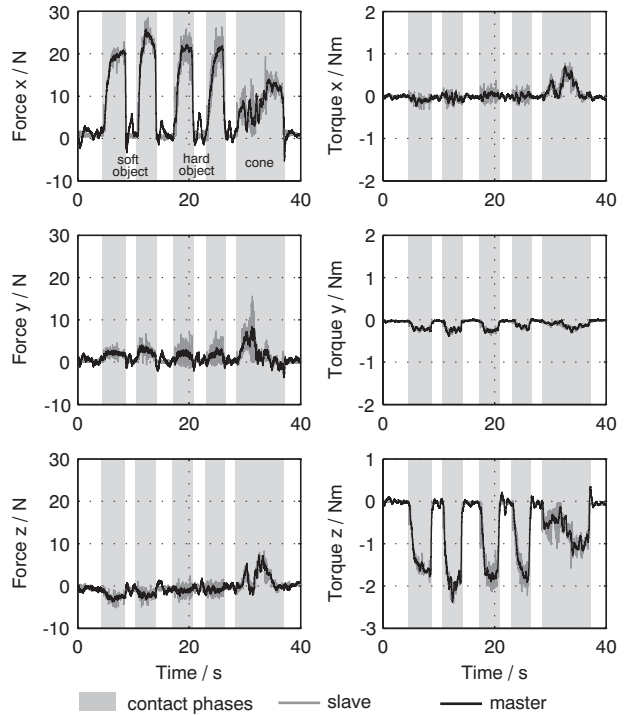


Fig.10: Force tracking (Master) during haptic exploration

REFERENCES

- [1] H. Baier, F. Freyberger, and G. Schmidt, "A high fidelity interactive stereo vision," in *Proceedings of the 2001 Workshop on Advances in Interactive Multimodal Telepresence Systems*, Munich, Germany, 2001, pp. 33–42.
- [2] B. Stanczyk and M. Buss, "Development of a telerobotic system for exploration of hazardous environments," in *Proc. IEEE Int. Conf. Intel. Rob. Syst. (IROS)*, Sendai, Japan, 2004.
- [3] F. Caccavale and B. Siciliano, "Quaternion-based kinematic control of redundant spacecraft/manipulator systems." in *ICRA*, 2001, pp. 435–440.
- [4] M. Ueberle, N. Mock, A. Peer, C. Michas, and M. Buss, "Design and Control Concepts of a Hyper Redundant Haptic Interface for Interaction with Virtual Environments," in *Proceedings of the IEEE/RSJ International Conference on Intelligent Robots and Systems IROS, Workshop on Touch and Haptics*, Sendai, Japan, 2004.
- [5] M. Ueberle and M. Buss, "Control of kinesthetic haptic interfaces," in *Proc. IEEE/RSJ Int. Conf. on Intellig. Rob. and Syst., Workshop on Touch and Haptics*, 2004.
- [6] P. Khosla and T. Kanade, "Real-time implementation of the computed-torque scheme," *IEEE Trans. Rob. Automat.*, vol. 5, no. 2, pp. 245–253, 1989.
- [7] A. Liégeois, "Automatic supervisory control of the configuration and behaviour of multibody mechanisms," *IEEE Tans. on Syst., Man, and Cybern.*, vol. 7, no. 12, pp. 868–871, 1977.
- [8] N. Nitzsche and G. Schmidt, "A Mobile Haptic Interface Mastering a Mobile Teleoperator," in *Proceedings of the IEEE/RSJ International Conference on Intelligent Robots and Systems IROS*, Sendai, Japan, 2004.
- [9] S. Hirche, B. Stanczyk, and M. Buss, "Transparent Exploration of Remote Environments by Internet Telepresence," in *Proceedings of Int. Workshop on High-Fidelity Telepresence and Teleaction jointly with the conference HUMANOIDS*, Munich, Germany, 2003.